Locating Sensors in Large-Scale Engineering Systems for Fault Isolation Based on Fault Feature Reduction

Jinxin Wang [a], Zhongwei Wang [a,] *, Xiuzhen Ma [a], Ann Smith [b], Fengshou Gu [b], Chi Zhang [a], Andrew Ball [b]

[a] *College of Power and Energy Engineering, Harbin Engineering University, Harbin 150001, China*

[b] *Centre for Efficiency and Performance Engineering, University of Huddersfield, Huddersfield HD1 3DH, UK*

Abstract: Fault detection and diagnosis (FDD) modules in a modern control system are effective in detecting and identifying abnormal process behaviours in a timely manner, ensuring the high-performance of large-scale engineering systems. The detection and isolation of faults is essentially built on the characterisation of the observed behaviour of a system. However, due to the large number of technical indicators available for measurement, as well as the various constraints of sensor installation, monitoring all the operating parameters of a large-scale engineering system is not feasible. Therefore, locating sensors optimally in a large-scale system, to achieve a comprehensive description of an abnormality, becomes a key issue to successfully apply diagnostic technologies to real world situations. In this paper, a fault feature reduction (FFR) based sensor location approach is proposed for optimal sensor placement so as to achieve the desired performance of fault detection and isolation. The behaviour of faults is firstly analysed using a fault tree to obtain a comprehensive understanding of the multi-dimensional relationships between faults and symptoms. A Boolean matrix is then constructed to represent the corresponding relations around faults and potential sensors. All the alternative configurations of sensors, for a desired diagnosis of a system, are obtained by eliminating the redundant fault features. The trade-off without a certain sensor is also attained using the

* Corresponding author.
Email addresses: wangjinxin@hrbeu.edu.cn (J. Wang), wangzw@hrbeu.edu.cn (Z. Wang), maxiuzhen@hrbeu.edu.cn (X. Ma), a.smith@hud.ac.uk (A. Smith), F.Gu@hud.ac.uk (F. Gu), zhangchi2018@hrbeu.edu.cn (C. Zhang), andrew.ball@hud.ac.uk (A. Ball).

following proposed approach. Three large-scale systems, including, a diesel engine system and two chemical systems, are used to illustrate the proposed approach. Comparisons to existing competitive techniques indicate the enhanced abilities of the proposed approach to meet the varying requirements of a real-world monitoring network. The analysis of sensor placement can be performed at the design phase of a large-scale engineering system, to locate the preset measured hole, or, during the life-cycle, to perfect an incomplete or redundant monitoring system.

Keywords: Large-scale engineering systems; Fault detection and diagnosis; Control system; Sensor location; Fault feature reduction

1. Introduction

Associated with the ever-increasing requirement for productivity and improved economic efficiency, the complexity and automaticity levels of engineering systems, e.g. mechanical systems and industrial systems, are continuously growing. These developing trends naturally ask for more stringent requirements for system safety and reliability. In order to maintain the high-performance of engineering systems, integrating the fault detection and diagnosis (FDD) module into a modern control system is highly desired.

Recent developments in signal processing, pattern recognition, controllers and their systematic integration have attractive potentials for resolving numerous issues related to FDD. Currently, most studies carried out in FDD field focuses on the failure mechanism [1,2], feature extraction [3-5] and fault identification and decision-making [6,7]. Locating sensors in a large-scale engineering system optimally, which is a

primary critical step for successful fault diagnostics, has not received the attention it deserves. Essentially, the detection and isolation of various faults is built on the characterisation of the observed behaviour of an engineering system [8]. Therefore, an accurate and comprehensive description of various faults is consequently considered to be the precondition for successful fault identification. Nevertheless, as for a real-world large-scale engineering system, there are usually tens or even hundreds of technical indicators available for measurement. Given the multiple constraints of monitoring cost and sensor installation, it is almost an unrealistic task to monitor all the operating parameters. Thus, effectively describing the systems behaviour using the least quantity of sensors is of great value for the fault diagnostics of a large-scale engineering system.

Some approaches have been developed to optimise the sensor location in a large-scale engineering system for dependable fault diagnostics. Generally, the sensor location approaches can be classified into three primary subcategories, i.e. reliability-based approach [9], observability-based approach [8-10] and isolatability-based approach (also known as resolution) [11-13]. The reliability-based approach designs a sensor network with redundancy to ensure a certain abnormality can be detected timely even in the case that some sensors are malfunctioned. Whilst this strategy maximises the reliability of condition

monitoring, the effective detection of every possible fault, however, cannot be guaranteed, which accordingly leads to a blind spot in the condition monitoring of a large-scale engineering system. This deficiency can be well tackled by locating sensors according to observability criterion. The sensor network complying with observability criterion makes all the potential faults observable by placing at least one sensor on their propagation paths. Therefore, an abnormality can be timely detected whenever the system undergoes a fault. However, for the successful application of fault diagnostics, it should not only be able to observe all the faults, but also separate and identify them to the maximum extent possible. To this end, the sensor location procedure for fault isolation is proposed. The strategy can give a quantity-optimum set of sensors that would be adequate to perform fault identification. Travé-Massuyès [14] proposes an algorithm for locating sensors based on a full diagnosability conception. Analytical redundancy relations (ARRs) derived from component-oriented models are utilised in their research to depict the causal dependency between faults (manifesting as the residuals of the redundancy relations) and the detectable parameters. The optimal configuration of sensors is obtained via traversing the alternative combinations of ARRs which involve all potential faults of interest. Although being well understood and fundamentally sound, it is a laborious and error-prone task to generate the detailed ARRs from an

exhaustive physics-based model, especially for large-scale nonlinear and/or dynamic systems. Take a diesel engine as an example, up to 1,640 ARRs can be generated from the 39 differential equations and algebraic equations (required to model the dynamic behaviours of the engine) to depict the dependency among the variables [15-17]. This incredible computational requirement brings considerable difficulties to applying the structural analysis-based approach to a high-complexity large-scale engineering system. Although some studies have been devoted to exploring ways to simply the procedure of structural analysis-based sensor location approach, e.g. coarse model [18] or bond-graph [13,19] for describing system behaviour, back substitution for generating ARRs [20], and dynamic programming for searching for optimal sensor sets [17], a higher-fidelity mathematical model of a large-scale engineering system is still needed for deriving the interactive relationship of a detector sensing a fault. This kind of model is not always available in the real-world and therefore limits these methods being widely applied in real-world situations.

An alternative view to optimise sensor placement is by means of graphical methods. Instead of ARRs, graphical methods exploit some cause-effect diagrams, e.g. signed directed graphs, process graphs and fault trees, to intuitively describe the effect of faults on multiple system variables. This capability makes the design of a sensor network in a

large-scale engineering system free from constructing a complex mathematical model. Lambert [21] analyses the causal relationships of faults and variables and hereby finds a feasible configuration of sensors to sense the target faults by means of a fault tree. Ali and Narasimhan [22,23] propose optimal strategies of sensor location in linear and bilinear systems respectively using process graphs analysis method. Various graph-theoretic concepts are used in [24] to configure the sensor location in a complex system. The approaches mentioned above fall into the reliability or observability category. The sensor location scheme using graphical method for the purpose of fault isolation is studied in [8]. The algorithms are well demonstrated through two widely used large-scale engineering systems, continuous stirred tank reactor (CSTR) and fluid catalytic cracking unit (FCCU). However, this approach can only obtain one possible configuration. In practice, a necessary sensor may not be installed due to the limitation of cost or installation space. In this situation, the alternative sensor placement solutions and the trade-off without this certain sensor are highly needed for operators. The approach in [8] cannot provide this information, which limits its applicability in real world.

In this paper, a novel fault feature reduction (FFR)-based sensor location methodology is proposed to achieve the desired performance of fault detectability and isolatability, by overcoming the deficiency of methods aforementioned. The causality between faults and symptoms of a

large-scale engineering system is firstly depicted using a fault tree. A Boolean matrix is constructed accordingly to represent the interactive relationship of a detector sensing a fault. The fewest-sensor subset is derived by eliminating the redundant sensors using a feature reduction method. The key contribution of this paper is summarised in: (i) the proposed FFR-based approach is technically implementable, which can be easily used in practice; (ii) all the possible configurations of sensors for a desired performance of fault isolatability that can be obtained; and (iii) the fault isolation ability without a certain sensor is also attained using the proposed approach, which gives a trade-off for the operators. The rest of this paper is organised as follows: Section 2 investigates the dependencies between faults and sensors by gradually elaborating the fault tree model of a large-scale engineering system. Section 3 presents an FFR-based approach for sensor location by taking a continuous stirred tank reactor as an example. A trade-off without a certain sensor is also provided in this section. Section 4 instantiates the proposed approach using a diesel engine and a fluid catalytic cracking unit. Finally, section 5 summarises the paper.

2. Extended Fault Tree for Causal Relationships Analysis

A sensor network which complies with fault isolatability criterion can be defined as follows.

Definition 2.1 A sensor network is designed using isolatability

criterion if and only if (i) for any logical combinations of sensor readings, at least one corresponding fault can be identified; and (ii) the abnormality caused by any a potential fault can be sensed via at least one placed sensor.

According to the definition above, the approach in this paper consists of 2 steps: (i) deriving the dependencies existing between faults and sensors; and (ii) eliminating the redundant sensors whilst keeping the capability for classifying pairs of faults unchanged. This section firstly exploits an extended fault tree to investigate the dependencies between faults and sensors of a large-scale engineering system.

In order to intuitively describe the approach, a continuous stirred tank reactor (CSTR) is taken as a demonstration to illustrate the procedure. A CSTR normally consists of a main reactor, a heat exchanger, a pump, and some control units, e.g. control valves, level temperature controllers. Main reactor is the core device which is equipped with an impeller or other mixing device to provide efficient mixing. The balance of reactor temperature and level in main reactor are achieved by reasonable control of the supplied coolant flow and the reactor output flow. In many research fields, CSTR is usually used as an example to exhibit the complex behavior such as steady-state multiplicity and limit cycles. Figure 1 shows the process diagram of a CSTR, for more details see [8,25]. The accident scenario of CSTR was analysed in detail by [8].

Table 1 presents the faults and sensors involved in the accident scenario, in which $f_1, f_2, \cdots, f_{13}$ represent the 13 potential faults of interest; while $s_1, s_2, \cdots, s_9$ denote the observable parameters which can be directly monitored via sensors (we do not differentiate observable parameters from sensors hereafter). It is worth noting that the faults and observable parameters in [8] are re-numbered, and the cycle existing in the CSTR process digraph is collapsed into a node L for a well-organised fault tree below. The accident scenario of CSTR is presented using fault tree by gradually elaborating the successions of undesired events until the final outcome. Since we try to obtain the causal relationships between faults and symptoms, the final outcome represents the observable parameters in this paper. Conventional fault tree can only describe the multiple-inputs-single-output logic. In practice, a fault may be characterised by only a single symptom, e.g. the leak of a pressure regulating valve of a diesel lubrication system can only be sensed via the pressure fluctuation of the main oil-gallery. To give full consideration of this realistic situation, the multiple-input-single-output logic gates (k : 1) assumption in a conventional fault tree is relaxed and extended to one-to-one input output gates (1 : 1). The extended fault tree of the CSTR is constructed as Figure 2. The extended gates (1 : 1) are utilised to describe the dependencies between $\mathrm{V_T}$ and F_W, and others.

205 Table 1

206 Common faults and sensors of a CSTR

Symbols	Faults	Symbols	Sensors
f_1	U	s_1	T_R
f_2	T_W	s_2	F_W
f_3	V_T	s_3	F_R
f_4	V_R	s_4	C_B
f_5	C_R	s_5	T
f_6	CA_0	s_6	TW_0
f_7	F_0	s_7	C_A
f_8	T_0	s_8	F_P
f_9	C_T	s_9	L
f_{10}	C_L		
f_{11}	V_L		
f_{12}	P_L		
f_{13}	P_P		

207

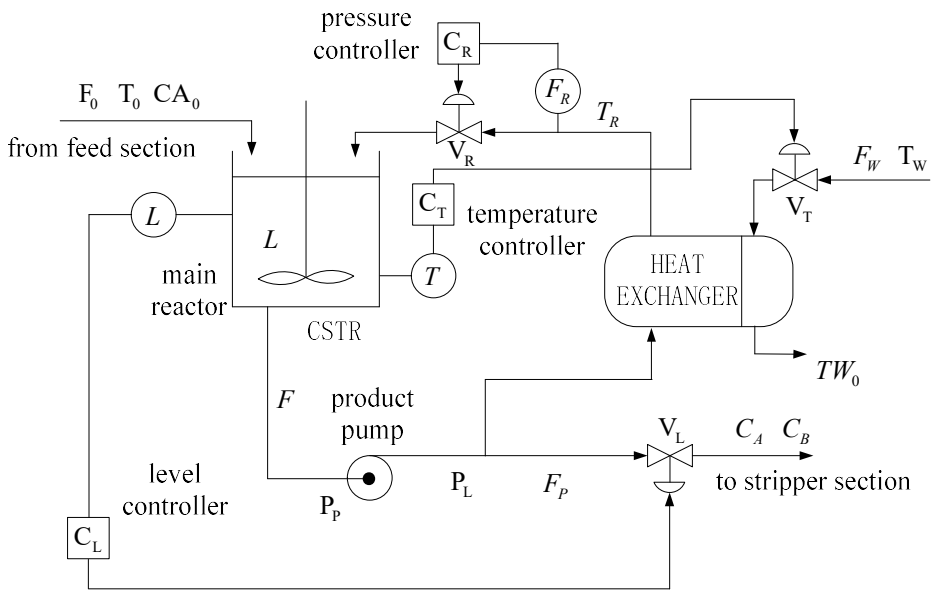

Figure 1: Process diagram of a CSTR

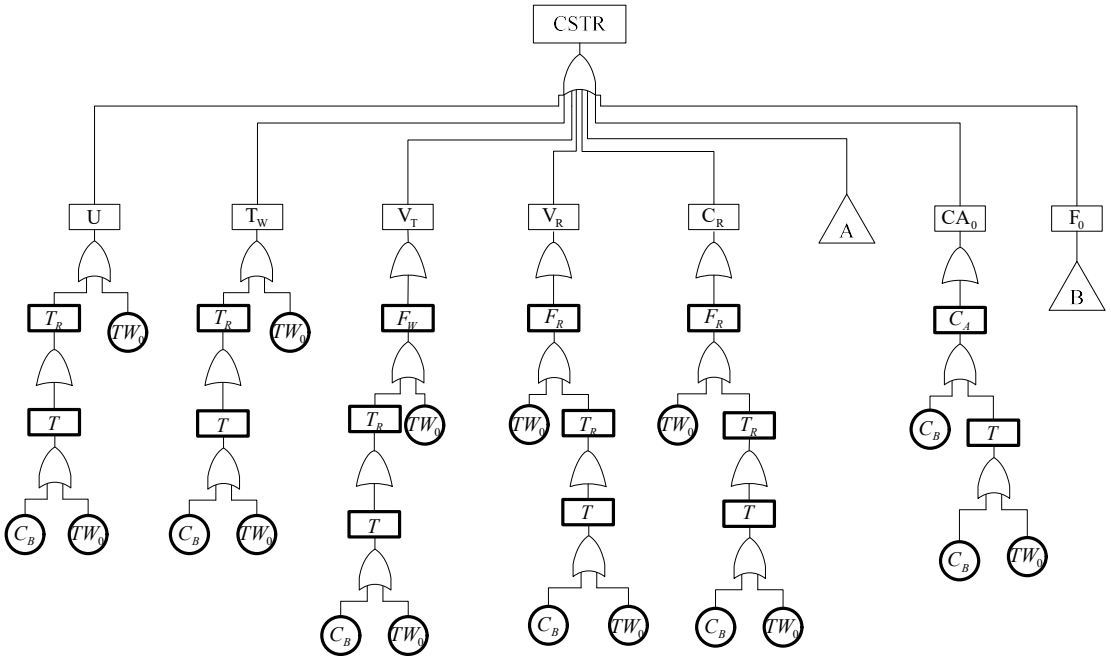

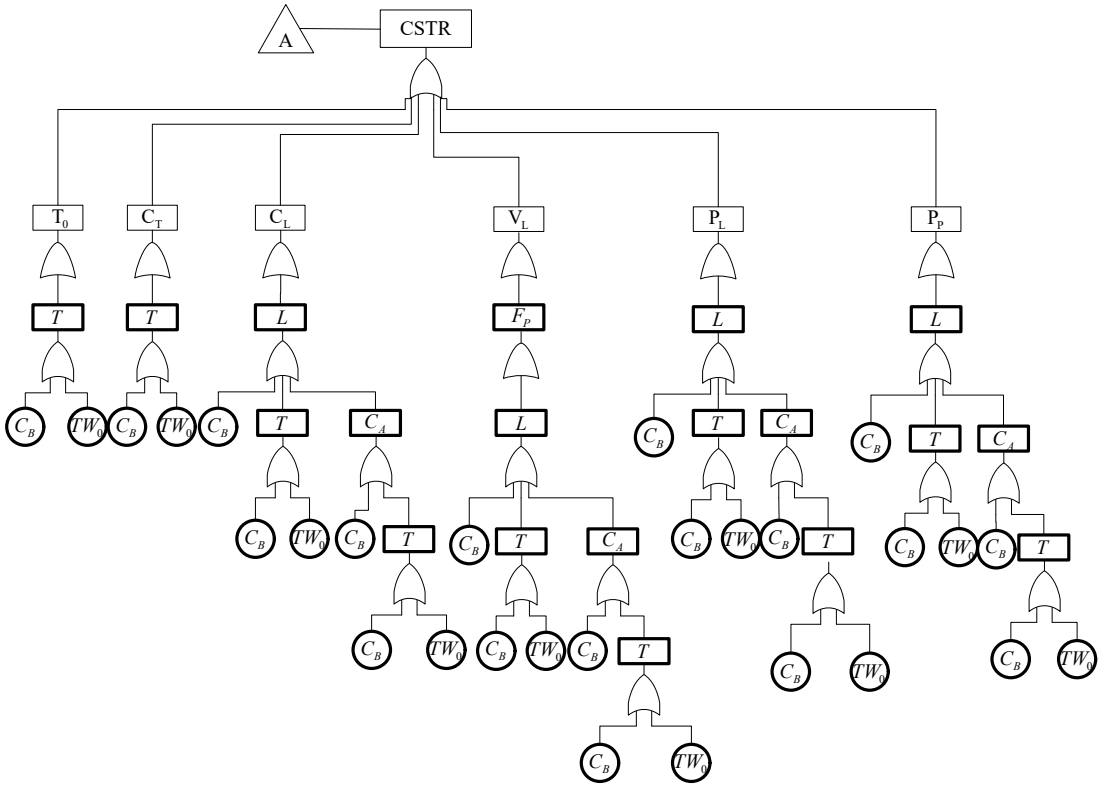

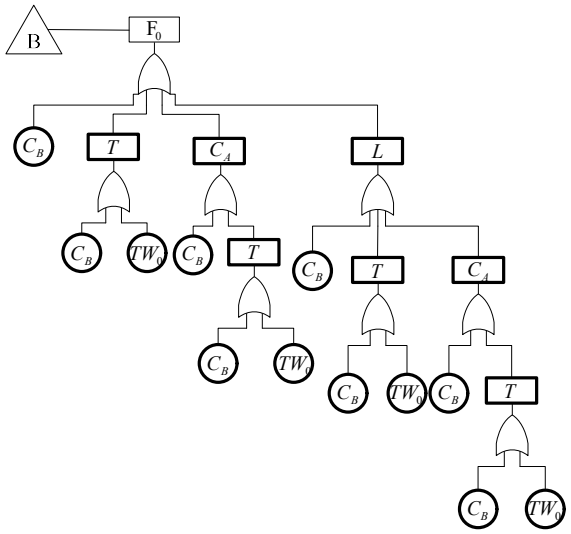

Figure 2: The fault tree of a CSTR

Fault tree intuitively presents which observable parameters would be affected if a fault presents. The causal relationships amongst faults and sensors can be visually described via a bipartite graph by removing the

sequentially dependent faults and unobservable parameters. The bipartite graph deriving from the fault tree of a CSTR is presented as Figure 3, in which the parents and children are instantiated as faults and sensors, respectively. A directed edge $f \to s$ exists if a fault f is perceived to be a direct cause of an abnormity s (or said sensed using a sensor s). The sensor location can be optimised after deriving the causal relationships.

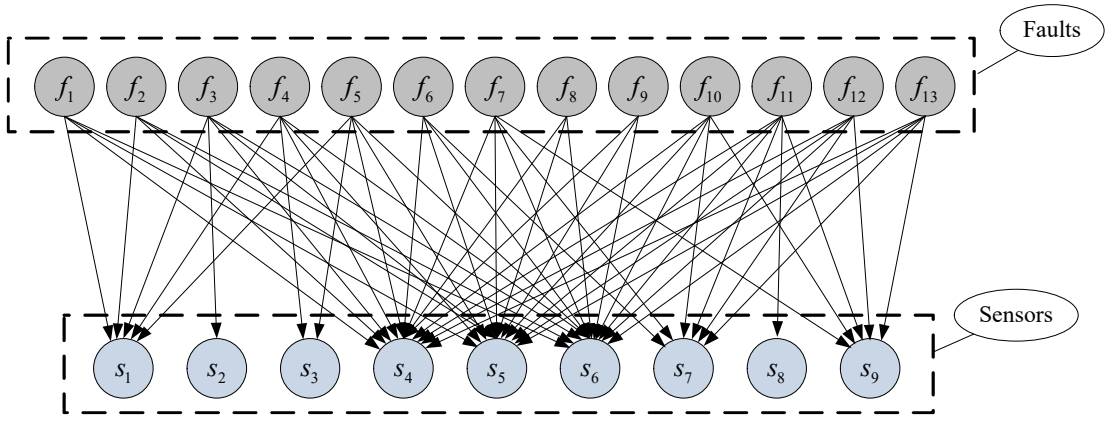

Figure 3: The bipartite graph of faults and sensors of a CSTR

3. Locating Sensors Based on Fault Feature Reduction (FFR)

3.1 Designing a complete sensor network by eliminating redundant sensors

Some fundamental concepts are firstly defined in this section to formulate the constraints imposed on the sensor placement.

Definition 3.1 Let $\Sigma = \langle F, S \rangle$ be a large-scale engineering system, in which $F = \{f_1, f_2, \cdots, f_n\}$ represents a set of interested faults and

$S=\{s_1,s_2,\cdots,s_k\}$ denotes a set of potential sensors. A *fault signature matrix* is defined as a Boolean matrix $\mathbf{M}(\Sigma)\in\{0,1\}^{n\times k}$, where $m_{ij}=1$ represents the fault f_i can be sensed via the sensor s_j, and $m_{ij}=0$ otherwise.

According to the definition, the row $r_i=(m_{ij})_{1\times k}$ of a *fault signature matrix* $\mathbf{M}(\Sigma)$ denotes all the alternative sensors for detecting the fault f_i. Let this set of sensors be $S_{fi}=\{s_j \mid s_j\in S\wedge m_{ij}=1\}$. Without loss of generality, it is assumed that all faults in a large-scale engineering system $\Sigma=\langle S,F\rangle$ are detectable, i.e. $r_i\neq(0)_{1\times k}$, $\forall i\in[1,n]\cap\mathbf{Z}^+$. Meanwhile, the exoneration working hypothesis is adopted in this paper, which means that the observable parameters will be always abnormal if the associated fault presents.

Given a *fault signature matrix* $\mathbf{M}(\Sigma)$, two faults f_i and f_j ($i\neq j$) are distinguishable if $m_{it}\neq m_{jt}$, $\exists s_t\in S'$, and indiscernible if $m_{it}=m_{jt}$, $\forall s_t\in S$. Using set partitioning concept [26], the following definition can be introduced.

Definition 3.2 Given a large-scale engineering system $\Sigma=\langle F,S\rangle$ and its *fault signature matrix* $\mathbf{M}(\Sigma)=(m_{ij})_{n\times k}$, name $[f_i]_{S'}$ an indiscernibility relation of fault f_i with a subset of sensors $S'\subseteq S$, where $[f_i]_{S'}=\{f_j \mid f_j\in F, m_{it}=m_{jt},\forall s_t\in S'\}$. The partition of F by S' is the set of the indiscernibility relation of all faults, i.e. $F/S'=\{[f_i]_{S'} \mid f_i\in F\}$.

Definition 3.2 tells how the faults are distinguished by a set of sensors. Based on this definition, a dispensable sensor can be defined as follows.

Definition 3.3 A sensor $s_t \in S$ is dispensable for fault isolation if and only if $F/S = F/S'$, $S' = S \setminus \{s_t\}$, where $S \setminus \{s_t\}$ denotes the subset of S after removing $\{s_t\}$.

A set of sensors S' is said quantity-optimum if all the sensors in S' are necessary to discern pairs of faults, i.e. no sensor is dispensable in S'.

Definition 3.4 Let $\Sigma = \langle F, S \rangle$ be a large-scale engineering system, the set of sensors $S' \subseteq S$ is a quantity-optimum set of sensors if $F/S' = F/S$ and $F/\left(S' \setminus \{s_t\}\right) \neq F/S$, $\forall s_t \in S'$.

According to the problem formulation above, locating a quantity-optimum set of sensors in a large-scale engineering system for fault isolation is therefore reformulated to the problem of eliminating the dispensable sensors. Given a large-scale engineering system $\Sigma = \langle F, S \rangle$ with n faults and k sensors, **Algorithm 1** is proposed to derive a quantity-optimum set of sensors for fault isolation.

Step 1 extend the *fault signature matrix* $\mathbf{M}(\Sigma)$ by adding a zero vector $r_{n+1} = \mathbf{0}_{1\times k}$ as the last row; treat the last row as a special fault f_{n+1};

Step 2 select a sensor s_t from S;

Step 3 if $F/\left(S \setminus \{s_t\}\right) = F/S$, then remove s_t from S;

Step 4 redo the steps above until all sensors have been selected, output the selected subset of sensors as S^*;

It is worth noting that the special fault f_{n+1} added in step 1 represents the normal condition of the engineering system. Since no parameter is abnormal when the system is in a good condition, the corresponding row vector is a zero vector. Therefore, step 1 makes all fault are observable.

As for the example of CSTR shown as Figure 1, the *fault signature matrix* can be generated according to the bipartite graph shown in Figure 3 as:

	s_1	s_2	s_3	s_4	s_5	s_6	s_7	s_8	s_9
f_1	1	0	0	1	1	1	0	0	0
f_2	1	0	0	1	1	1	0	0	0
f_3	1	1	0	1	1	1	0	0	0
f_4	1	0	1	1	1	1	0	0	0
f_5	1	0	1	1	1	1	0	0	0
f_6	0	0	0	1	1	1	1	0	0
f_7	0	0	0	1	1	1	1	0	1
f_8	0	0	0	1	1	1	0	0	0
f_9	0	0	0	1	1	1	0	0	0
f_{10}	0	0	0	1	1	1	1	0	1
f_{11}	0	0	0	1	1	1	1	1	1
f_{12}	0	0	0	1	1	1	1	0	1
f_{13}	0	0	0	1	1	1	1	0	1

Figure 4: The fault signature matrix of a CSTR

Given the complete set of sensors $S=\{s_1,\cdots,s_9\}$, the partition of $F=\{f_1,\cdots,f_{13}\}$ can be calculated as

$$F/S=\{\{f_1,f_2\},\{f_3\},\{f_4,f_5\},\{f_6\},\{f_7,f_{10},f_{12},f_{13}\},\{f_8,f_9\},\{f_{11}\}\}$$

Each element in the quotient set F/S denotes the faults that cannot be distinguished using any sensor in S. Using **Algorithm 1**, the sensors $\{s_4,s_5\}$ are identified as the dispensable sensors since removing them does not alter the partition of F. Sensor s_6 is retained in the quantity-optimum sensor network after extending the *fault signature matrix* $\mathbf{M}(\Sigma)$ for the observability of faults f_8 as well as f_9. Therefore, the sensors set $S^*=\{s_1,s_2,s_3,s_6,s_7,s_8,s_9\}$ is the optimal one to isolate multiple faults of a CSTR. Raghuraj [8] makes use of CSTR to demonstrate their algorithms for sensor location. The result derived from **Algorithm 1** is consistent with [8], which indicates that the proposed approach can effectively find a quantity-optimum set of sensors so as to achieve the desired performance of fault detectability and isolatability.

In practice, it is necessary to know all alternative sensor placement solutions to give the operators various options. The alternative solutions can be obtained by enumerating all possible combinations of candidate sensors. However, this strategy will become intractable when tens of sensors available for condition monitoring (known as NP-hard problem). **Algorithm 1** is found limited to derive all feasible sensor placement solutions. In the following, a more fruitful approach for deducing all the

optimal configurations of sensors is proposed.

According to the definition above, set $S_{fi}=\left\{s_j \middle| s_j \in S \wedge m_{ij}=1\right\}$ denotes all the alternative sensors for detecting the fault f_i. Consequently, every single non-empty element s_t contained in the symmetric difference of S_{fi} and S_{fj}, i.e. $s_t \in \Delta S_{fi,fj}=\left\{S_{fi} \cup S_{fj}\right\} \setminus \left\{S_{fi} \cap S_{fj}\right\}$, represents the necessary sensor that is sufficient to distinguish fault f_i from f_j. The optimisation of sensor location can therefore be pursued via generating the symmetric difference of pairs of faults and then combining the non-empty elements using Boolean logic. This purpose is realised by instantiating the concept of a *discernibility matrix* [27].

Definition 3.5 Let $\mathbf{M}(\Sigma) \in \{0,1\}^{n \times k}$ be the *fault signature matrix* of a large-scale engineering system $\Sigma=\langle F,S\rangle$ as definition 3.1. Its *discernibility matrix* is defined as $\mathbf{D}(\Sigma)=\left\{\Delta S_{fi,fj}\right\}^{n \times n}$, $i, j \in [1,n] \cap \mathbf{Z}^{+}$.

The elements in $\mathbf{D}(\Sigma)$ store the sets of sensors which are enough to discern pairs of faults. All the alternative combinations of sensors for fault isolation can be derived via the Boolean calculation of the $\Delta S_{fi,fj}$ using *discernibility function* $f(\Sigma)$.

$$f(\Sigma)=\wedge\left\{\vee s \middle| s \in \Delta S_{fi,fj}, \Delta S_{fi,fj} \neq \varnothing\right\} \tag{1}$$

where $\vee s$ is the disjunction of sensors s such that $s \in \Delta S_{fi,fj}$; $\wedge s$ is the conjunctive of s.

Each conjunctive form in the minimal disjunctive normal form of

$f(\Sigma)$ presents a feasible sensor placement solution for the purpose of fault isolation. Thus, a modified algorithm to derive all alternative sensor placement solutions, that is **Algorithm 2**, is given as follows.

Step 1 generate a *fault signature matrix* $\mathbf{M}(\Sigma)$ of a large-scale engineering system Σ according to the dependencies between faults and sensors;

Step 2 extend the *fault signature matrix* $\mathbf{M}(\Sigma)$ by adding a zero vector $r_{n+1}=\mathbf{0}_{1\times k}$ as the last row; treat the last row as a special fault f_{n+1};

Step 3 deduce the *discernibility matrix* $\mathbf{D}(\Sigma)$ from the *fault signature matrix* $\mathbf{M}(\Sigma)$;

Step 4 calculate the *discernibility function* $f(\Sigma)$ by combining the non-empty elements in the *discernibility matrix* $\mathbf{D}(\Sigma)$ using Boolean logic;

Step 5 output each conjunctive form in the minimal disjunctive normal form of $f(\Sigma)$ as a feasible solution S^* for sensor placement.

For the example of CSTR, the *discernibility matrix* $\mathbf{D}(\Sigma)$ of the extended *fault signature matrix* $\mathbf{M}(\Sigma)$ can be calculated from definition 3.5 as follows. It is clear that the *discernibility matrix* $\mathbf{D}(\Sigma)$ is a symmetric matrix. Therefore, the *discernibility matrix* $\mathbf{D}(\Sigma)$ is presented as an upper triangular matrix in this paper.

$$\mathbf{D}(\Sigma)=\begin{bmatrix}
\phi & \phi & \{s_2\} & \{s_3\} & \{s_3\} & \{s_1,s_7\} & \{s_1,s_7,s_9\} & \{s_1\} & \{s_1\} & \{s_1,s_7,s_9\} & \{s_1,s_7,s_8,s_9\} & \{s_1,s_7,s_9\} & \{s_1,s_7,s_9\} & \{s_1,s_4,s_5,s_6\} \\
 & \phi & \{s_2\} & \{s_3\} & \{s_3\} & \{s_1,s_7\} & \{s_1,s_7,s_9\} & \{s_1\} & \{s_1\} & \{s_1,s_7,s_9\} & \{s_1,s_7,s_8,s_9\} & \{s_1,s_7,s_9\} & \{s_1,s_7,s_9\} & \{s_1,s_4,s_5,s_6\} \\
 & & \phi & \{s_2,s_3\} & \{s_2,s_3\} & \{s_1,s_2,s_7\} & \{s_1,s_2,s_7,s_9\} & \{s_1,s_2\} & \{s_1,s_2\} & \{s_1,s_2,s_7,s_9\} & \{s_1,s_2,s_7,s_8,s_9\} & \{s_1,s_2,s_7,s_9\} & \{s_1,s_2,s_7,s_9\} & \{s_1,s_2,s_4,s_5,s_6\} \\
 & & & \phi & \phi & \{s_1,s_3,s_7\} & \{s_1,s_3,s_7,s_9\} & \{s_1,s_3\} & \{s_1,s_3\} & \{s_1,s_3,s_7,s_9\} & \{s_1,s_3,s_7,s_8,s_9\} & \{s_1,s_3,s_7,s_9\} & \{s_1,s_3,s_7,s_9\} & \{s_1,s_3,s_4,s_5,s_6\} \\
 & & & & \phi & \{s_1,s_3,s_7\} & \{s_1,s_3,s_7,s_9\} & \{s_1,s_3\} & \{s_1,s_3\} & \{s_1,s_3,s_7,s_9\} & \{s_1,s_3,s_7,s_8,s_9\} & \{s_1,s_3,s_7,s_9\} & \{s_1,s_3,s_7,s_9\} & \{s_1,s_3,s_4,s_5,s_6\} \\
 & & & & & \phi & \{s_9\} & \{s_7\} & \{s_7\} & \{s_9\} & \{s_8,s_9\} & \{s_9\} & \{s_9\} & \{s_4,s_5,s_6,s_7\} \\
 & & & & & & \phi & \{s_7,s_9\} & \{s_7,s_9\} & \phi & \{s_8\} & \phi & \phi & \{s_4,s_5,s_6,s_7,s_9\} \\
 & & & & & & & \phi & \phi & \{s_7,s_9\} & \{s_7,s_8,s_9\} & \{s_7,s_9\} & \{s_7,s_9\} & \{s_4,s_5,s_6\} \\
 & & & & & & & & \phi & \{s_7,s_9\} & \{s_7,s_8,s_9\} & \{s_7,s_9\} & \{s_7,s_9\} & \{s_4,s_5,s_6\} \\
 & & & & & & & & & \phi & \{s_8\} & \phi & \phi & \{s_4,s_5,s_6,s_7,s_9\} \\
 & & & & & & & & & & \phi & \{s_8\} & \{s_8\} & S\setminus\{s_1,s_2,s_3\} \\
 & & & & & & & & & & & \phi & \phi & \{s_4,s_5,s_6,s_7,s_9\} \\
 & & & & & & & & & & & & \phi & \{s_4,s_5,s_6,s_7,s_9\} \\
 & & & & & & & & & & & & & \phi
\end{bmatrix}$$

The *discernibility function* $f(\Sigma)$ and the minimal disjunctive normal form can be easily deduced from the matrix $\mathbf{D}(\Sigma)$ as

$$f(\Sigma)=s_1s_2s_3s_4s_7s_8s_9+s_1s_2s_3s_5s_7s_8s_9+s_1s_2s_3s_6s_7s_8s_9$$

Therefore, the optimal sensor placement solutions which guarantee the observability and isolatability of all fualts are listed as follows.

$$S_1^*=\{s_1,s_2,s_3,s_4,s_7,s_8,s_9\}$$

$$S_2^*=\{s_1,s_2,s_3,s_5,s_7,s_8,s_9\}$$

$$S_3^*=\{s_1,s_2,s_3,s_6,s_7,s_8,s_9\}$$

The sets of sensors S_1^*, S_2^*, and S_3^* show all alternative configuration of sensors for complete fault isolation. The multiple solutions give the operators various options to select. The operators can choose any a solution according to their need while keeping the capability for fault isolation unchanged.

3.2 The fault coverage rate of an incomplete sensor network

In practice, an existing sensor network may be imperfect, or a

necessary sensor cannot be equipped due to the various constraints of sensor installation. Once a sensor network is found incomplete, it is necessary to know which faults cannot be identified with the existing sensors or the sensors planned to be installed. In this section, the evaluation of an incomplete sensor network is discussed. The trade-off without a certain sensor is provided accordingly.

Given a set of sensors S', a large-scale engineering system Σ is fully isolatable if $\forall i, j \in [1, n] \cap \mathbf{Z}^+$, $i \neq j$, $r_i \neq r_j$, where r_i, r_j are rows of the corresponding *fault signature matrix* $\mathbf{M}(\Sigma)$. System Σ is partially isolatable if $\exists i, j \in [1, n] \cap \mathbf{Z}^+$, $i \neq j$, $r_i = r_j$. For an engineering system Σ in real-world, the maximum isolatable fault that can be achieved essentially depends on the characteristics of the engineering system. Some faults are inherently indistinguishable given any possible sensors, e.g. in the example of CSTR, faults f_1 and f_2 cannot be isolated even given the complete set of sensors S; so as $\{f_4, f_5\}$, $\{f_8, f_9\}$, and $\{f_7, f_{10}, f_{12}, f_{13}\}$. Thus, the maximum isolatable fault on an engineering system is implicitly assumed to be attained with a complete set of sensors. Consequently, instead of using the absolute isolation of faults, it is more reasonable to evaluate a sensor network using the relative value. In this paper, *fault coverage rate* is defined to quantify the performance of a sensor network.

Definition 3.6 Let $\Sigma = \langle F, S \rangle$ be a large-scale engineering system.

The *fault coverage rate* c of a set of sensors $S' \subseteq S$ is defined as

$$c = \frac{|F/S'|}{|F/S|} \times 100\%$$

where $|\cdot|$ denotes the operator of cardinal number of a set.

Travé-Massuyès [14] proposed an approach for calculating the absolute maximum of fault isolation in an engineering system based on *structural rank*. This indicator can be more easily calculated using definition 3.2 and definition 3.6. The *fault coverage rate* c of a quantity-optimum set of sensors is certainly 100% since it has the complete capability for fault isolation as the original one. Sensors which exist in all possible solutions of sensor network are called *core sensors*. In the case of a CSTR, the *core sensor set* is $S_{core} = S_1^* \bigcap S_2^* \bigcap S_3^* = \{s_1, s_2, s_3, s_7, s_8, s_9\}$. The *core sensors* are indispensable to distinguish pairs of faults. Some distinguishable faults will become indistinguishable without the *core sensors*. Suppose that sensor s_1 is absent in a sensor network whilst others are present, i.e. $S' = \{s_2, s_3, s_4, s_5, s_6, s_7, s_8, s_9\}$. The partition of F is therefore calculated as $F/S' = \{\{f_1, f_2, f_8, f_9\}, \{f_3\}, \{f_4, f_5\}, \{f_6\}, \{f_7, f_{10}, f_{12}, f_{13}\}, \{f_{11}\}\}$. Comparing with the indiscernibility relation by S, it shows that faults f_8 and f_9 cannot be distinguished from f_1 and f_2 without s_1. The *fault coverage rate* without sensor s_1 can be calculated accordingly as $c = 85.71\%$. It shows that absence of s_1 decreases the ability of fault isolation.

The *non-core sensors* can be replaced by other sensors while does not decrease the *fault coverage rate*. It can be seen that sensor s_4 can be replaced by sensor s_5 and s_6 without a decrease in the *fault coverage rate*. Therefore, the partition of F and *fault coverage rate* describe the contribution of a sensor with regard to fault isolation. They consequently provide a trade-off as to whether a sensor should be configured given the contribution of that sensor and the constraints of installation.

4. Case Study

In this section, two cases, i.e. a diesel engine and a Fluid Catalytic Cracking Unit (FCCU), are used to present a complete procedure of sensor location. The approach is compared to existing competitive techniques to illustrate the enhanced abilities for real-world application.

4.1 Sensor location in a diesel engine

Case 1 is used to illustrate the advantages using isolatability-based sensor placement approach compared with an observability-based approach. The sensor location problem of a diesel engine was studied in [28] using an observability-based approach. According to their research, the common faults and observable parameters are presented in Table 2. The dependencies between faults and symptoms are presented in Table 3.

442 Table 2

443 Common faults and parameters of a diesel engine

Symbols	Faults	Symbols	Observable Parameters
f_1	Misfire	s_1	Cylinder pressure
f_2	Cylinder score	s_2	Acoustic emission signal
f_3	Fault in fuel injector	s_3	Emission concentration
f_4	Crankshaft crack	s_4	Lubricant monitoring index
f_5	Fault in crankshaft bearing	s_5	Torsional vibration of crankshaft
f_6	Fault in piston pin	s_6	Noise signal
f_7	Improper injection timing	s_7	Oil mist
f_8	Poor fuel atomization	s_8	Fuel supply pressure
f_9	Cylinder blow-by	s_9	Surface temperature of engine
f_{10}	Insufficient air intake	s_{10}	Ultrasonic signal
f_{11}	Fault in air valve	s_{11}	Instantaneous speed
		s_{12}	Cylinder head vibration

444

445 Table 3

446 The fault signature matrix of a diesel engine

	s_1	s_2	s_3	s_4	s_5	s_6	s_7	s_8	s_9	s_{10}	s_{11}	s_{12}
f_1	1	0	0	0	1	1	0	0	0	0	1	1
f_2	0	1	0	1	1	0	1	0	0	0	0	0
f_3	1	0	1	0	1	1	0	1	0	0	1	1
f_4	0	1	0	1	1	0	0	0	0	0	0	0

f_5	0	1	0	0	0	1	0	0	1	0	0	1
f_6	0	0	0	0	0	1	0	0	1	0	0	1
f_7	1	0	0	0	0	1	0	1	0	0	1	1
f_8	1	0	0	0	0	1	1	1	0	0	1	1
f_9	1	0	0	0	0	1	0	1	0	1	1	1
f_{10}	1	0	0	0	0	1	0	1	0	0	0	1
f_{11}	0	0	0	0	0	0	0	0	0	0	1	1

The causal relationships presented in Table 3 can be depicted intuitively as Figure 5. Based on the bipartite graph, the faults of diesel engine $F=\{f_1,\cdots,f_{11}\}$ are partitioned completely by the observable parameters, as:

$$F/S=\{\{f_1\},\{f_2\},\{f_3\},\{f_4\},\{f_5\},\{f_6\},\{f_7\},\{f_8\},\{f_9\},\{f_{10}\},\{f_{11}\}\}$$

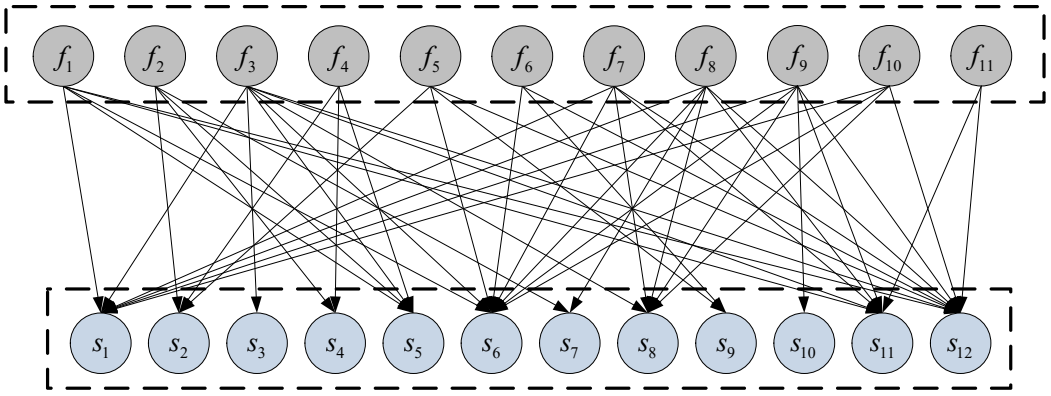

Figure 5: The bipartite graph of a diesel engine

Algorithm 1 is used respectively to design a sensor network of the

458 diesel engine for the purpose of fault isolation. Table 4 compares the
459 sensor network derived using **Algorithm 1** with the result in [28].

460

461 Table 4

462 Comparisons of the sensor networks complying with reliability and observability

463 criteria and FFR

Details	The method in [28]	Algorithm 1
Number of sensors	2	7
Sensor positions	s_5, s_{12}	$s_2, s_5, s_7, s_8, s_{10}, s_{11}, s_{12}$
Indistinguishable faults	$\{f_1, f_3\}$, $\{f_2, f_4\}$ and $\{f_5, f_6, f_7, f_8, f_9, f_{10}, f_{11}\}$	none
fault coverage rate	27.27%	100%

464

465 In [28], sensors *torsional vibration of crankshaft* s_5 and *cylinder*
466 *head vibration* s_{12} are selected to monitor the health condition of diesel
467 engines. Although all faults can be detected using s_5 and s_{12}, the *fault*
468 *coverage rate* of $S^* = \{s_5, s_{12}\}$ is calculated as 27.27%, which shows the
469 limitation for fault isolation. Specifically, faults $\{f_1, f_3\}$, $\{f_2, f_4\}$ and
470 $\{f_5, f_6, f_7, f_8, f_9, f_{10}, f_{11}\}$ cannot be distinguished from each other using
471 $S^* = \{s_5, s_{12}\}$ since the element value in the fault signature matrix
472 corresponding to $S^* = \{s_5, s_{12}\}$ are same with each other. Using
473 **Algorithm 1**, $S^* = \{s_2, s_5, s_7, s_8, s_{10}, s_{11}, s_{12}\}$ is derived as the
474 quantity-optimum set of sensors for the purpose of fault isolation. The
475 *fault coverage rate* of S^* is calculated as 100%, which means the subset
476 S^* has the same capacity to distinguish pairs of faults as the original one.

The quantity of sensors for fault isolation is reduced from 12 to 7 using the proposed approach which decreases the difficulty and cost of diesel engine condition monitoring.

4.2 Sensor location in a FCCU

Fluid catalytic cracking units are one of the most vital systems in the petroleum industry. A fluid catalytic cracking unit usually consists of several components, including a feed and preheats system, a reactor, a regenerator, air blowers, a main fractionator and wet gas compressor. Figure 6 shows the schematic flow diagram of a typical fluid catalytic cracking unit based on a “side-by-side” configuration [29]. The procedure of sensor location for an entire FCCU cannot be presented completely due to space limitations. The reactor, which is considered to be the most important component in FCCU, is taken as an example to illustrate the sensor location approach.

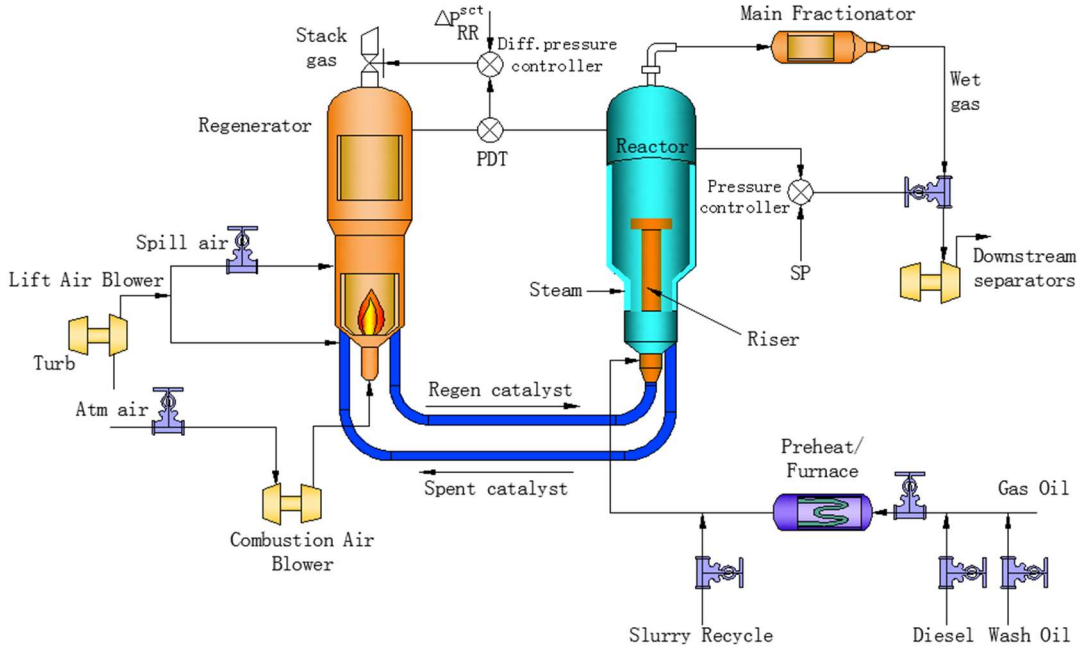

Figure 6: A fluid catalytic cracking unit with a “side-by-side” configuration

Mylaraswamy [30] analysed the causal relationships of the reactor by taking advantage of CATSIM, which is a dynamic simulation for the Amoco Model IV Fluid Catalytic Cracking Unit. Table 5 presents the common events in the troubleshooting of the reactor. The events symbolized with f in Table 5 represent the faults of a reactor. Table 6 presents the related observable parameters, which are corresponding to different sensors for measurement. Accordingly to the causal relationships described in [30], the fault tree of a reactor is constructed as Figure 7.

Table 5

Common events in the troubleshooting of a reactor

Symbols	Events	Symbols	Events

f_1	Flow of fresh feed to reactor riser	f_{13}	Wet gas flare valve flow rating
f_2	Flow-rate of regenerated catalyst	f_{14}	Flow through wet gas compressor anti-surge valve
f_3	Flow of wash oil to reactor riser	f_{15}	Temperature of fresh feed entering reactor riser
f_4	Flow of diesel oil to reactor riser	f_{16}	Enthalpy of regenerated catalyst
f_5	Effective coke factor for gas-oil feed	m_1	Enthalpy into regenerator, reactor
f_6	Height of reactor riser	m_2	Inventory of catalyst in reactor
f_7	Flow-rate of spent catalyst	m_3	Inventory of catalyst in reactor riser
f_8	Flow of slurry to reactor riser	m_4	Catalyst residence time in riser
f_9	Weight fraction of coke on regenerated catalyst	m_5	Weight hourly space velocity
f_{10}	Flow through wet gas compressor suction valve	m_6	Volumetric flow-rate in reactor riser
f_{11}	Atmospheric pressure	m_7	Average density of material in reactor riser
f_{12}	Wet gas flare valve position (0-1)		

Table 6

The observable parameters of a reactor

Symbols	Observable parameters	Symbols	Observable parameters
s_1	Effect of feed type on coke production	s_6	Wet gas production in reactor
s_2	Production of coke in reactor riser	s_7	Pressure at bottom of reactor riser
s_3	Weight fraction of coke on spent catalyst	s_8	Reactor pressure
s_4	Temperature of spent catalyst entering regenerator	s_9	Reactor fractionator pressure
s_5	Temperature of reactor riser		

511

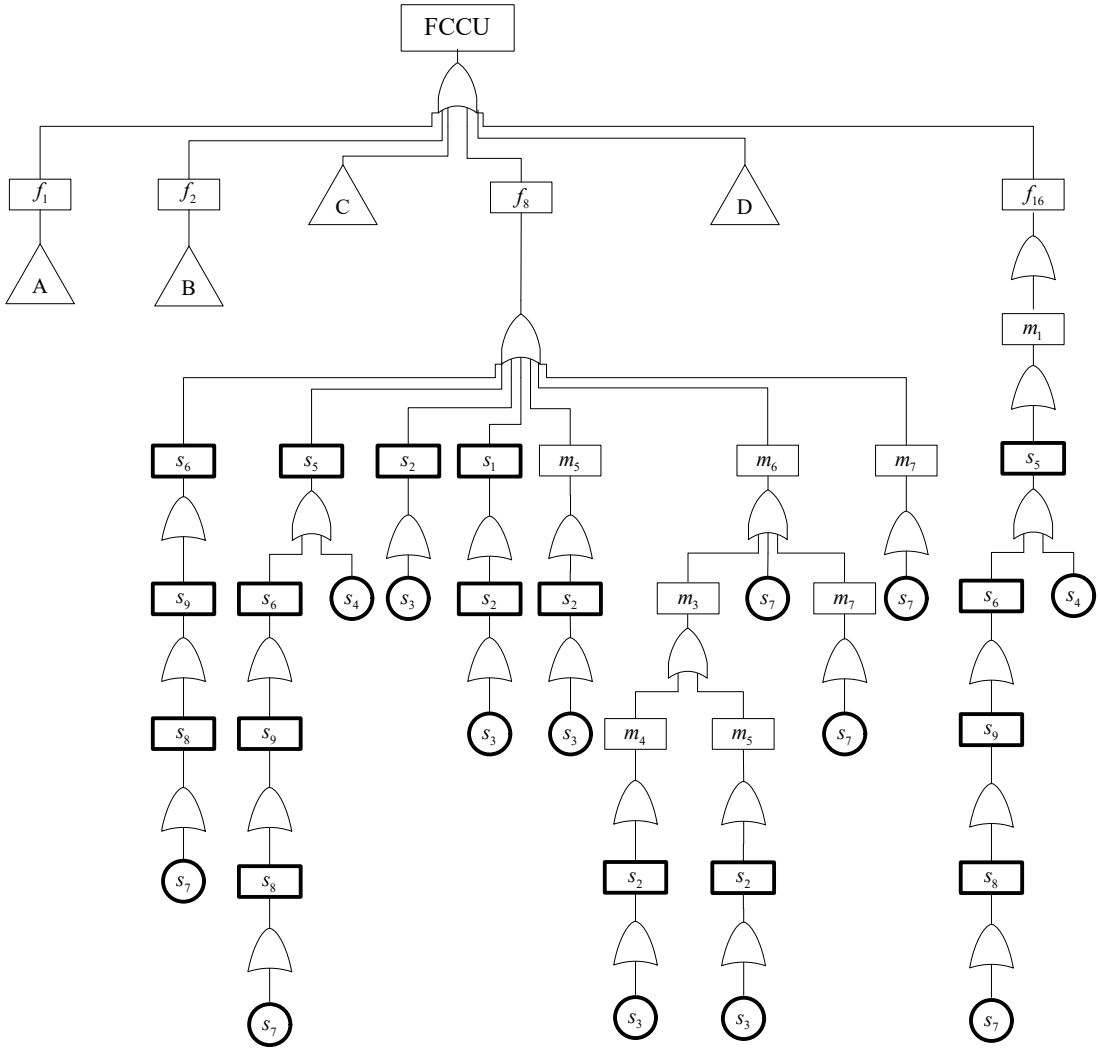
FCCU
f_1
f_2
C
f_8
D
f_{16}
A
B
m_1
s_6
s_5
s_2
s_1
m_5
m_6
m_7
s_5
s_9
s_6
s_4
s_3
s_2
s_2
m_3
s_7
m_7
s_7
s_6
s_4
s_8
s_9
s_3
s_3
m_4
m_5
s_7
s_9
s_7
s_8
s_2
s_2
s_8
s_7
s_3
s_3
s_7

512

513

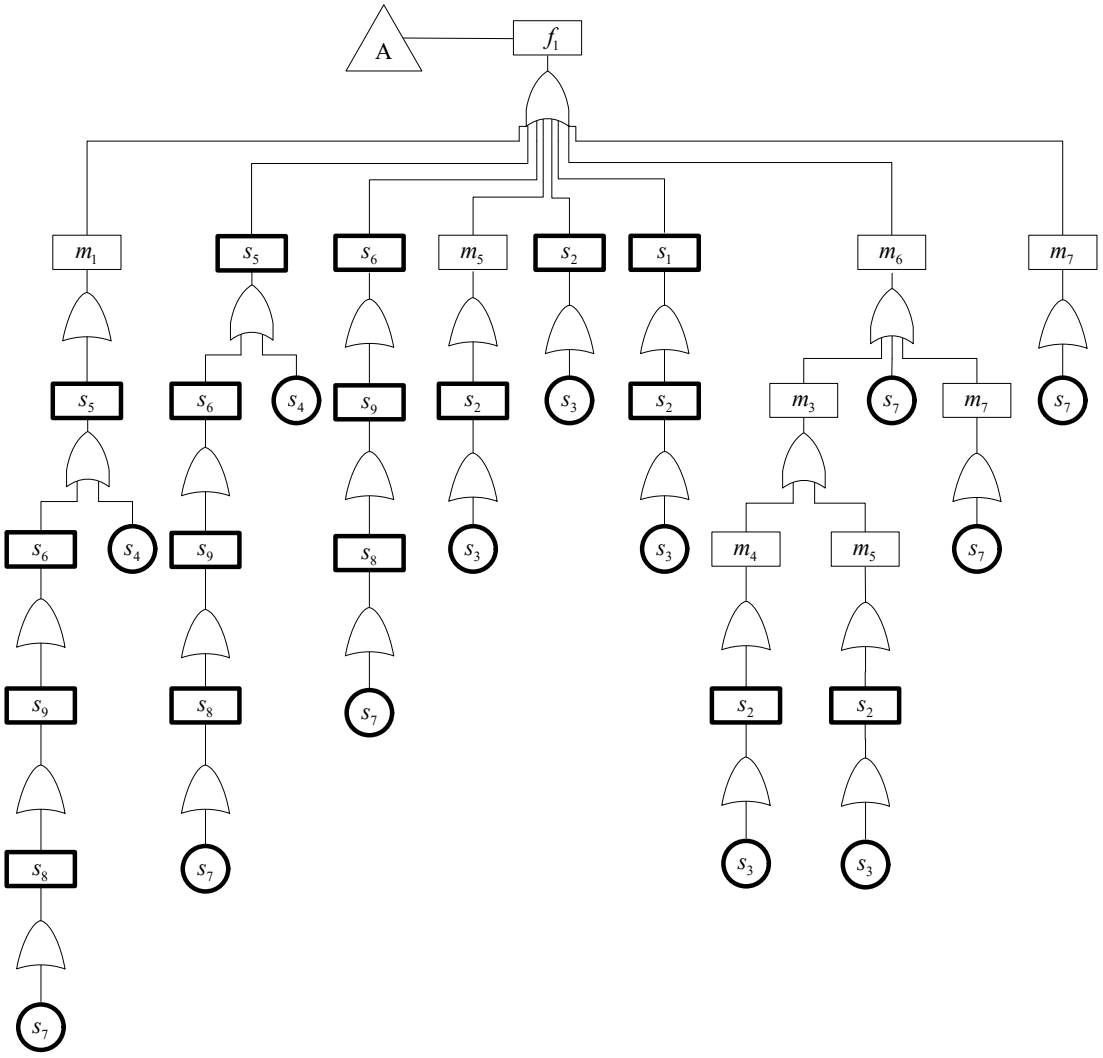
A
f_1
m_1
s_5
s_6
s_4
s_9
s_8
s_7
s_4
s_9
s_8
s_7
s_6
s_9
s_8
s_7
m_5
s_2
s_3
s_2
s_3
s_1
s_2
s_3
m_6
m_3
s_7
m_4
s_2
s_3
m_5
s_2
s_3
m_7
s_7
m_7
s_7
s_7

514

515

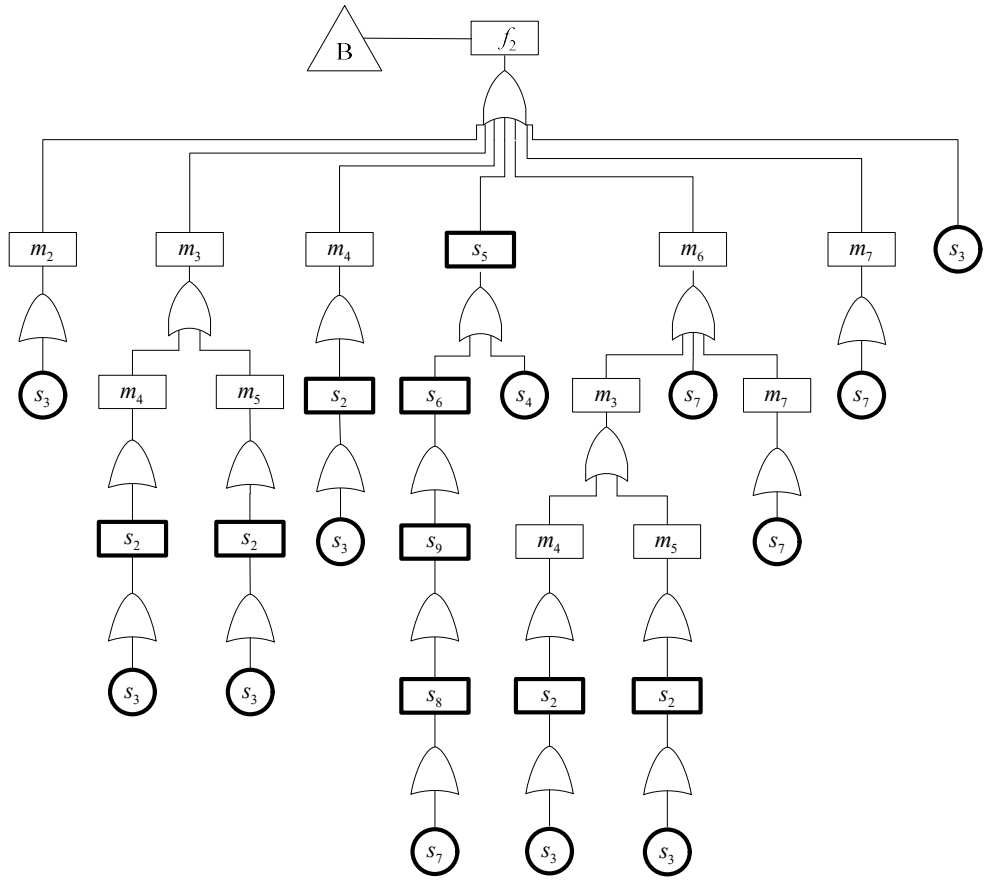
B
f_2
m_2
m_3
m_4
s_5
m_6
m_7
s_3
s_3
m_4
m_5
s_2
s_6
s_4
m_3
s_7
m_7
s_7
s_2
s_2
s_3
s_9
m_4
m_5
s_7
s_3
s_3
s_8
s_2
s_2
s_7
s_3
s_3

516

517

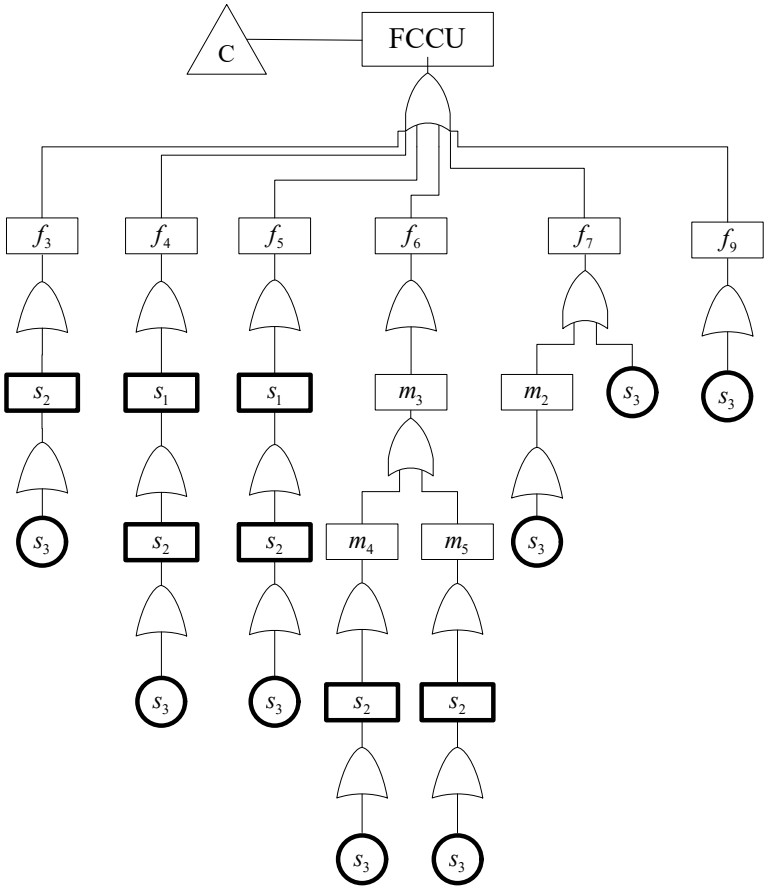
C
FCCU
f_3
f_4
f_5
f_6
f_7
f_9
s_2
s_1
s_1
m_3
m_2
s_3
s_3
s_3
s_2
s_2
m_4
m_5
s_3
s_3
s_3
s_2
s_2
s_3
s_3

518

519

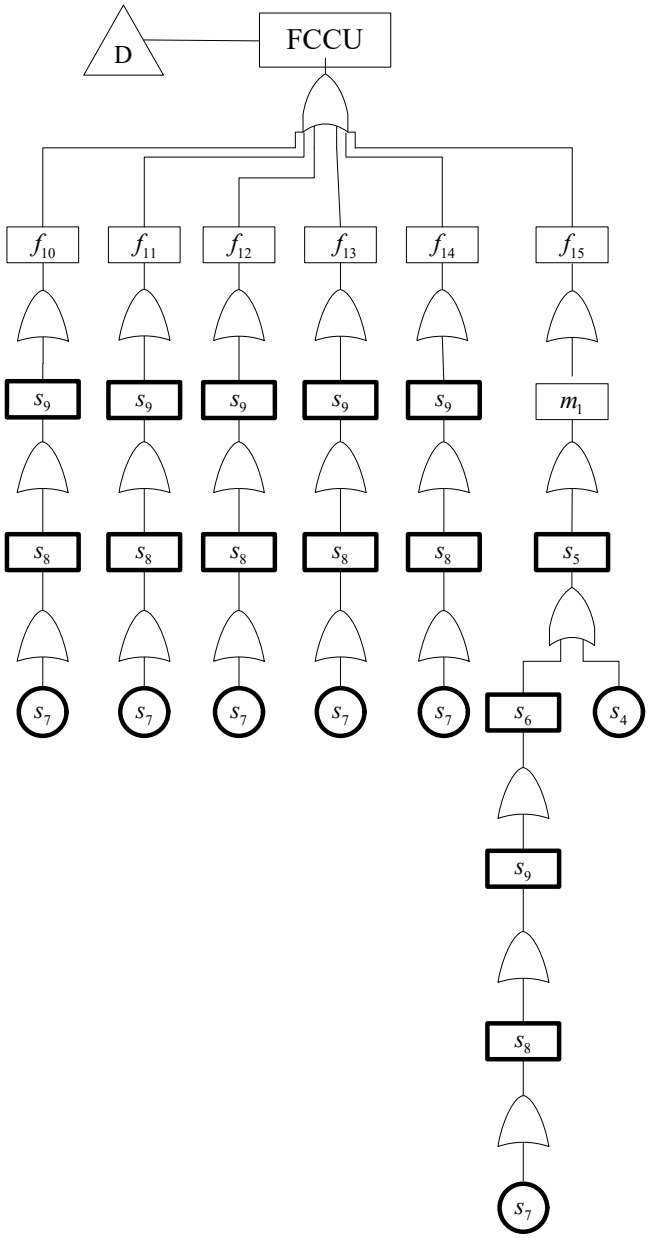

Figure 7: The fault tree of a FCCU

From the extended fault tree, we can construct a bipartite graph of faults and sensors of the reactor as Figure 8.

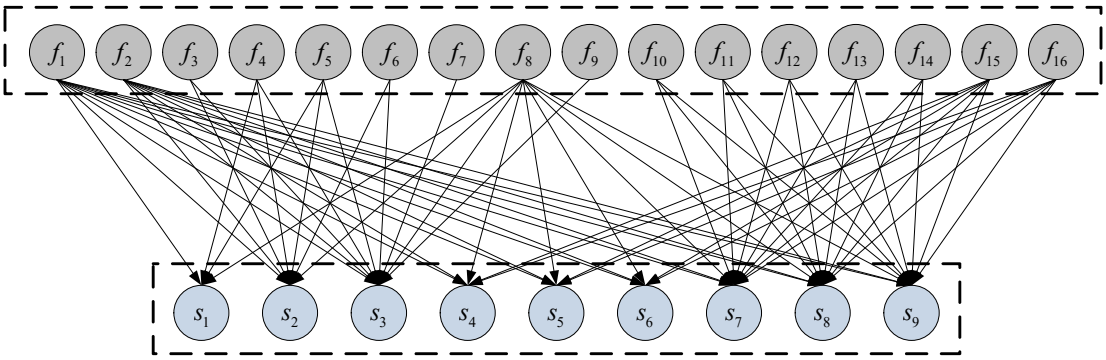

Figure 8: The bipartite graph of a FCCU

The dependencies of faults and sensors of a reactor presented in Figure 8 can be described using a *fault signature matrix* which is given in Table 7.

Table 7

The fault signature matrix of a reactor

	s_1	s_2	s_3	s_4	s_5	s_6	s_7	s_8	s_9
f_1	1	1	1	1	1	1	1	1	1
f_2	0	1	1	1	1	1	1	1	1
f_3	0	1	1	0	0	0	0	0	0
f_4	1	1	1	0	0	0	0	0	0
f_5	1	1	1	0	0	0	0	0	0
f_6	0	1	1	0	0	0	0	0	0
f_7	0	0	1	0	0	0	0	0	0
f_8	1	1	1	1	1	1	1	1	1
f_9	0	0	1	0	0	0	0	0	0

f_{10}	0	0	0	0	0	0	1	1	1
f_{11}	0	0	0	0	0	0	1	1	1
f_{12}	0	0	0	0	0	0	1	1	1
f_{13}	0	0	0	0	0	0	1	1	1
f_{14}	0	0	0	0	0	0	1	1	1
f_{15}	0	0	0	1	1	1	1	1	1
f_{16}	0	0	0	1	1	1	1	1	1

The partition of $F=\{f_1,\cdots,f_{16}\}$ by a complete set of sensors S can be calculated as:

$$F/S=\{\{f_1,f_8\},\{f_2\},\{f_3,f_6\},\{f_4,f_5\},\{f_7,f_9\},\{f_{10},f_{11},f_{12},f_{13},f_{14}\},\{f_{15},f_{16}\}\}$$

It shows that faults $\{f_1,f_8\}$, $\{f_3,f_6\}$, $\{f_4,f_5\}$, $\{f_7,f_9\}$, $\{f_{10},f_{11},f_{12},f_{13},f_{14}\}$ and $\{f_{15},f_{16}\}$ are inherently indistinguishable using any sensors. **Algorithm 1** is firstly used to design the sensor network. The result is presented in Table 8, Column 3. According to **Algorithm 1**, sensors $S^*=\{s_1,s_2,s_3,s_6,s_9\}$ are selected as the quantity-optimum sensor network for FCCU fault isolation. The partition of $F=\{f_1,\cdots,f_{16}\}$ by S^*, i.e. F/S^*, is calculated as equal to F/S, therefore the sensor network S^* has fully capability of distinguishing the multiple faults as the original sensor network S. The sensor network constructed in [8] is also presented in Table 8. The sensor network derived using **Algorithm 1** is consistent with the conclusion in [8], which validates the proposed

549 approach. It should be noted the faults and observable parameters are
550 renumbered compared with [8] for a well-organised graphical model. The
551 quantity of sensors for FCCU fault isolation is reduced from 9 to 5
552 compared with the original sensor network, which makes the condition
553 monitoring of a FCCU easy to be implemented in practice.

554 **Algorithm 2** is then utilised to seek all alternative sensor
555 configurations. The *discernibility matrix* $\mathbf{D}(\Sigma)$ of the extended *fault*
556 *signature matrix* $\mathbf{M}(\Sigma)$ is derived using definition 3.5. Since the
557 *discernibility matrix* $\mathbf{D}(\Sigma)$ has a high order of 17, i.e.
558 $\mathbf{D}(\Sigma)=\left\{\Delta S_{fi,fj}\right\}^{17\times 17}$, for a succinct description, the matrix $\mathbf{D}(\Sigma)$ is
559 represented as a block matrix, that is

560 $$\mathbf{D}(\Sigma)=\begin{bmatrix}\mathbf{D}_{11}(\Sigma) & \mathbf{D}_{12}(\Sigma)\\ \mathbf{D}_{21}(\Sigma) & \mathbf{D}_{22}(\Sigma)\end{bmatrix}$$

561 where

562 $$\mathbf{D}_{11}(\Sigma)=\begin{bmatrix}
\phi & \{s_1\} & S\setminus\{s_2,s_3\} & S\setminus\{s_1,s_2,s_3\} & S\setminus\{s_1,s_2,s_3\} & S\setminus\{s_2,s_3\} & S\setminus\{s_3\} & \phi & S\setminus\{s_3\}\\
 & \phi & S\setminus\{s_1,s_2,s_3\} & S\setminus\{s_2,s_3\} & S\setminus\{s_2,s_3\} & S\setminus\{s_1,s_2,s_3\} & S\setminus\{s_1,s_3\} & \{s_1\} & S\setminus\{s_1,s_3\}\\
 & & \phi & \{s_1\} & \{s_1\} & \phi & \{s_2\} & S\setminus\{s_2,s_3\} & \{s_2\}\\
 & & & \phi & \phi & \{s_1\} & \{s_1,s_2\} & S\setminus\{s_1,s_2,s_3\} & \{s_1,s_2\}\\
 & & & & \phi & \{s_1\} & \{s_1,s_2\} & S\setminus\{s_1,s_2,s_3\} & \{s_1,s_2\}\\
 & & & & & \phi & \{s_2\} & S\setminus\{s_2,s_3\} & \{s_2\}\\
 & & & & & & \phi & S\setminus\{s_3\} & \phi\\
 & & & & & & & \phi & S\setminus\{s_3\}\\
 & & & & & & & & \phi
\end{bmatrix}$$

563

564 $$\mathbf{D}_{12}(\Sigma)=\begin{bmatrix} S\setminus\{s_7,s_8,s_9\} & S\setminus\{s_7,s_8,s_9\} & S\setminus\{s_7,s_8,s_9\} & S\setminus\{s_7,s_8,s_9\} & S\setminus\{s_7,s_8,s_9\} & \{s_1,s_2,s_3\} & \{s_1,s_2,s_3\} & S \\ \{s_2,s_3,s_4,s_5,s_6\} & \{s_2,s_3,s_4,s_5,s_6\} & \{s_2,s_3,s_4,s_5,s_6\} & \{s_2,s_3,s_4,s_5,s_6\} & \{s_2,s_3,s_4,s_5,s_6\} & \{s_2,s_3\} & \{s_2,s_3\} & S\setminus\{s_1\} \\ \{s_2,s_3,s_7,s_8,s_9\} & \{s_2,s_3,s_7,s_8,s_9\} & \{s_2,s_3,s_7,s_8,s_9\} & \{s_2,s_3,s_7,s_8,s_9\} & \{s_2,s_3,s_7,s_8,s_9\} & S\setminus\{s_1\} & S\setminus\{s_1\} & \{s_2,s_3\} \\ S\setminus\{s_4,s_5,s_6\} & S\setminus\{s_4,s_5,s_6\} & S\setminus\{s_4,s_5,s_6\} & S\setminus\{s_4,s_5,s_6\} & S\setminus\{s_4,s_5,s_6\} & S & S & \{s_1,s_2,s_3\} \\ S\setminus\{s_4,s_5,s_6\} & S\setminus\{s_4,s_5,s_6\} & S\setminus\{s_4,s_5,s_6\} & S\setminus\{s_4,s_5,s_6\} & S\setminus\{s_4,s_5,s_6\} & S & S & \{s_1,s_2,s_3\} \\ \{s_2,s_3,s_7,s_8,s_9\} & \{s_2,s_3,s_7,s_8,s_9\} & \{s_2,s_3,s_7,s_8,s_9\} & \{s_2,s_3,s_7,s_8,s_9\} & \{s_2,s_3,s_7,s_8,s_9\} & S\setminus\{s_1\} & S\setminus\{s_1\} & \{s_2,s_3\} \\ \{s_3,s_7,s_8,s_9\} & \{s_3,s_7,s_8,s_9\} & \{s_3,s_7,s_8,s_9\} & \{s_3,s_7,s_8,s_9\} & \{s_3,s_7,s_8,s_9\} & S\setminus\{s_1,s_2\} & S\setminus\{s_1,s_2\} & \{s_3\} \\ S\setminus\{s_7,s_8,s_9\} & S\setminus\{s_7,s_8,s_9\} & S\setminus\{s_7,s_8,s_9\} & S\setminus\{s_7,s_8,s_9\} & S\setminus\{s_7,s_8,s_9\} & \{s_1,s_2,s_3\} & \{s_1,s_2,s_3\} & S \\ \{s_3,s_7,s_8,s_9\} & \{s_3,s_7,s_8,s_9\} & \{s_3,s_7,s_8,s_9\} & \{s_3,s_7,s_8,s_9\} & \{s_3,s_7,s_8,s_9\} & S\setminus\{s_1,s_2\} & S\setminus\{s_1,s_2\} & \{s_3\} \end{bmatrix}$$

565

566 $$\mathbf{D}_{21}(\Sigma)=[\ ]_{8\times 9}$$

567 $$\mathbf{D}_{22}(\Sigma)=\begin{bmatrix} \phi & \phi & \phi & \phi & \phi & \{s_4,s_5,s_6\} & \{s_4,s_5,s_6\} & \{s_7,s_8,s_9\} \\ & \phi & \phi & \phi & \phi & \{s_4,s_5,s_6\} & \{s_4,s_5,s_6\} & \{s_7,s_8,s_9\} \\ & & \phi & \phi & \phi & \{s_4,s_5,s_6\} & \{s_4,s_5,s_6\} & \{s_7,s_8,s_9\} \\ & & & \phi & \phi & \{s_4,s_5,s_6\} & \{s_4,s_5,s_6\} & \{s_7,s_8,s_9\} \\ & & & & \phi & \{s_4,s_5,s_6\} & \{s_4,s_5,s_6\} & \{s_7,s_8,s_9\} \\ & & & & & \phi & \phi & S\setminus\{s_1,s_2,s_3\} \\ & & & & & & \phi & S\setminus\{s_1,s_2,s_3\} \\ & & & & & & & \phi \end{bmatrix}$$

568 The *discernibility function* $f(\Sigma)$ of a reactor and the minimal
569 disjunctive normal form are then deduced, and the quantity-optimum sets
570 of sensors for the fault isolation of a reactor in a FCCU can be listed as
571 follows.

572 $$S_1^*=\{s_1,s_2,s_3,s_4,s_7\},\ \ S_2^*=\{s_1,s_2,s_3,s_4,s_8\},\ \ S_3^*=\{s_1,s_2,s_3,s_4,s_9\}$$

573 $$S_4^*=\{s_1,s_2,s_3,s_5,s_7\},\ \ S_5^*=\{s_1,s_2,s_3,s_5,s_8\},\ \ S_6^*=\{s_1,s_2,s_3,s_5,s_9\}$$

574 $$S_7^*=\{s_1,s_2,s_3,s_6,s_7\},\ \ S_8^*=\{s_1,s_2,s_3,s_6,s_8\},\ \ S_9^*=\{s_1,s_2,s_3,s_6,s_9\}$$

575 Table 8 presents the quantity-optimum sensor networks designed
576 using **Algorithm 2**.

577

578 Table 8

579 Comparisons of the sensor networks designed using different approaches

Details	Graphical method in [8]	Algorithm 1	Algorithm 2

Number of sensors	5	5	5
Sensor positions	s_1, s_2, s_3, s_6, s_9	s_1, s_2, s_3, s_6, s_9	s_1, s_2, s_3, s_4, s_7 s_1, s_2, s_3, s_4, s_8 s_1, s_2, s_3, s_4, s_9 s_1, s_2, s_3, s_5, s_7 s_1, s_2, s_3, s_5, s_8 s_1, s_2, s_3, s_5, s_9 s_1, s_2, s_3, s_6, s_7 s_1, s_2, s_3, s_6, s_8 s_1, s_2, s_3, s_6, s_9
Indistinguishable faults	$\{f_1, f_8\}, \{f_3, f_6\}$ $\{f_4, f_5\}, \{f_7, f_9\}$ $\{f_{10}, f_{11}, f_{12}, f_{13}, f_{14}\}$ $\{f_{15}, f_{16}\}$	$\{f_1, f_8\}, \{f_3, f_6\}$ $\{f_4, f_5\}, \{f_7, f_9\}$ $\{f_{10}, f_{11}, f_{12}, f_{13}, f_{14}\}$ $\{f_{15}, f_{16}\}$	$\{f_1, f_8\}, \{f_3, f_6\}$ $\{f_4, f_5\}, \{f_7, f_9\}$ $\{f_{10}, f_{11}, f_{12}, f_{13}, f_{14}\}$ $\{f_{15}, f_{16}\}$
fault coverage rate	100%	100%	100%

Algorithm 2 derives all possible combinations of sensors for a desired performance of fault detectability and isolation. The multiple quantity-optimum sets of sensors provide various options to design sensor networks for fault isolation of a reactor. The contribution of each sensor can also be quantified using this approach to facilitate the assessment as to whether a sensor should be configured or not. The *core sensor set* is $S_{core} = S_1^* \cap \cdots \cap S_9^* = \{s_1, s_2, s_3\}$. Now consider sensor s_1 cannot be installed in a FCCU due to the space limitation, i.e. $S' = \{s_2, s_3, s_6, s_9\}$. Using definition 3.6 and definition 3.2, the *fault coverage rate* is calculated as $c = |F/S'| / |F/S| = 71.43\%$, and the partition of F is

$F/S' = \{\{f_1, f_2, f_8\}, \{f_3, f_4, f_5, f_6\}, \{f_7, f_9\}, \{f_{10}, f_{11}, f_{12}, f_{13}, f_{14}\}, \{f_{15}, f_{16}\}\}$.

Therefore, some faults cannot be distinguished from each other without sensor s_1, e.g. fault f_2 is recognised as the same category with $\{f_1, f_8\}$ without sensor s_1 therefore fault f_2 cannot be identified using $S' = \{s_2, s_3, s_6, s_9\}$. The result gives the operators how severe it is without a certain sensor, and therefore helps the operators to decide whether to install a certain sensor.

5. Discussion

The proposed approach firstly uses different characters (0 and 1) to represent the different influence the faults on the sensor readings, and then select the quantity-optimum set of sensors according to these characters. The potential future improvements can be listed as follows.

(1) Different faults may have different effects on the sensed variables, e.g. opposite effects. Given this situation, various characters can be used to sign these effects. As for the opposite effects, the *fault signature matrix* can be extended by using "-1" denote the negative influence, "1" represents the positive influence, and "0" represents there is no influence. **Algorithm 1** and **Algorithm 2** can be naturally extended for these situations.

(2) As for multiple-fault assumption, the multiple or simultaneous faults can be viewed as a special fault, which has the influence on the all

sensors that are corresponding to each single faults. Therefore, **Algorithm 1** and **Algorithm 2** are still applicative for sensor placement under multiple-fault assumption.

(3) Although all sensor placement solution derived from the proposed approach are enough for fault isolation, different solutions vary in case of cost, install space or fault isolation accuracy (if taking sensor accuracy into consideration). Therefore, it is desired to know which solution is the most needed one. This problem can be viewed as the follow-up step after getting all feasible solutions, and optimisation algorithms can be used to search the optimal solution.

6. Conclusions

This paper proposes a novel approach to locate sensors in a large-scale engineering system for fault isolation based on FFR. This approach firstly takes use of an extended fault tree to capture the multi-dimensional causal relationships between faults and symptoms. All alternative configurations of sensors for a desired diagnosability of a system are then obtained by eliminating the redundant fault features. Three large-scale systems are used as examples to illustrate the proposed approach. Results show that the FFR-based approach reduces the quantity of sensors from 9 to 7 as for the CSTR system, from 12 to 7 as for a diesel engine, and from 9 to 5 as for a FCCU, which facilitate the

condition monitoring of a large-scale engineering system. Besides, the proposed approach can derive all the alternative configurations of sensors for a desired diagnosability of a system, and provide the trade-off without a certain sensor. This helps operators to make an informed decision regarding sensor placement. This approach can be utilised at the design phase of a large-scale engineering system, to locate the preset measured hole, or, during the life-cycle, to perfect an incomplete or a redundant monitoring system.

Acknowledgements

This research is financially supported by The National Natural Science Fund of China (Grant No: 51305089) and Natural Science Foundation of Heilongjiang Province of China (Grant No: E2016018).

References

[1] X. Liang, M. J. Zuo, Z. Feng, Dynamic modeling of gearbox faults: a review, Mech Syst Signal Pr 98 (2018) 852-876.

[2] H. Towsyfyan, F. Gu, A. Ball, B. Liang, Modelling acoustic emissions generated by tribological behaviour of mechanical seals for condition monitoring and fault detection, Tribol Int 125 (2018) 46-58.

[3] S. Zhang, Q. He, K. Ouyang, W. Xiong, Multi-bearing weak defect detection for wayside acoustic diagnosis based on a time-varying spatial filtering rearrangement, Mech Syst Signal Pr 100 (2018) 224-241.

[4] L. Hu, L. Zhang, F. Gu, N. Hu, A. Ball, Extraction of the largest amplitude impact transients for diagnosing rolling element defects in bearings, Mech Syst Signal Pr 116 (2019) 796-815.

[5] W. Li, C. Zhao, Hybrid fault characteristics decomposition based probabilistic distributed fault diagnosis for large-scale industrial processes, Control Eng Pract 84 (2019) 377-388.

[6] R. Venkataraman, P. Bauer, P. Seiler, B. Vanek, Comparison of fault detection and isolation methods for a small unmanned aircraft, Control Eng Pract 84 (2019) 365-376.

[7] B. Cai, Y. Liu, M. Xie, A dynamic-bayesian-network-based fault diagnosis methodology considering transient and intermittent faults, IEEE T Autom Sci Eng 14 (1) (2017) 276-285.

[8] R. Raghuraj, M. Bhushan, R. Rengaswamy, Locating sensors in complex chemical plants based on fault diagnostic observability criteria, AIChE J 45 (2) (1999) 310-322.

[9] R. Duan, Y. Lin, T. Feng, Optimal sensor placement based on system reliability criterion under epistemic uncertainty, IEEE Access 6 (2018) 57061-57072.

[10] S. Sahoo, X. Yin, J. Liu, Optimal sensor placement for agro-hydrological systems. AIChE J 65 (12) (2019) 1-18.

[11] C. Chen, L. Chen, J. Ding, Y. Wu, The effectivity analysis of adding sensors for improving model based fault isolability properties. J. Process Contr 70 (2018) 123-132.

[12] L. S. Perelman, W. Abbas, X. Koutsoukos, S. Amin, Sensor placement for fault location identification in water newtorks: a minimum test cover approach, Automatica 72 (2016) 166-176.

[13] G. Chi, D. Wang, Sensor placement for fault isolability based on bond graphs, IEEE T Automat Contr 60 (11) (2015) 3041-3046.

[14] L. Travé-Massuyès, T. Escobet, X. Olive, Diagnosability analysis based on component-supported analytical redundancy relations, IEEE T Syst Man Cy-S 36 (6) (2006) 1146-1160.

[15] J. Wahlström, L. Eriksson, Modelling diesel engines with a variable-geometry turbocharger and exhaust gas recirculation by optimization of model parameters for capturing non-linear system dynamics, P I of Mech Eng 225 (7) (2011)

960-986.

[16] C. Svärd, M. Nyberg, E. Frisk, M. Krysander, Automotive engine FDI by application of an automated model-based and data-driven design methodology, Control Eng Pract 21 (4) (2013) 455-472.

[17] G. Chi, D. Wang, T. Le, M. Yu, M. Luo, Sensor placement for fault isolability using low complexity dynamic programming, IEEE T Autom Sci Eng 12 (3) (2015) 1080-1091.

[18] M. Krysander, E. Frisk, Sensor placement for fault diagnosis, IEEE T Syst Man Cy-S 38 (6) (2008) 1398-1410.

[19] M. Khemliche, B. O. Bouamama, H. Haffaf, Sensor placement for component diagnosability using bond-graph, Sensor Actuat 132 (2) (2006) 547-556.

[20] A. Rosich, E. Frisk, J. Åslund, R. Sarrate, F. Nejjari, Fault diagnosis based on causal computations, IEEE T Syst Man Cy-S 42 (2) (2012) 371-381.

[21] H.E. Lambert, Fault trees for locating sensors in process systems, Chem Eng Prog August (1977) 81-85.

[22] Y. Ali, S. Narasimhan, Redundant sensor network design for linear processes, AIChE J 41 (10) (1995) 2237-2249.

[23] Y. Ali, S. Narasimhan, Sensor network design for maximizing reliability of bilinear processes, AIChE J 42 (9) (1996) 2563-2575.

[24] S. Sen, S. Narasimhan, K. Deb, Sensor network design of linear processes using genetic algorithms, Comput Chem Eng 22 (3) (1998) 385-390.

[25] H. Shi, P. Li, J. Cao, C. Su, J. Yu, Robust fuzzy predictive control for discrete-time systems with interval time-varying delays and unknown disturbances, IEEE Trans Fuzzy Syst. 2019, DOI: 10.1109/TFUZZ.2019.2959539

[26] M. Wolski, A. Gomolinska, Data meaning and knowledge discovery: Semantical aspects of information systems, Int J Approx Reason 119 (2020) 40-57.

[27] J. Wang, Y. Qian, F. Li, J. Liang, W. Ding. Fusing fuzzy monotonic decision trees, IEEE Trans Fuzzy Syst. 2019, DOI: 10.1109/TFUZZ.2019.2953024

[28] P. Yan, X. Huang, G. Lian, Y. Zhang, Research on multi-class sensor placement optimisation method for fault diagnosis of mechanical power and transmission

719 system based on fault-sensor dependence matrix, Comput Meas Control 20 (7)
720 (2012) 1753-1756.
721 [29] A. Golrokh Sani, H. Ale Ebrahim, M. J. Azarhoosh, 8-Lump kinetic model for
722 fluid catalytic cracking with olefin detailed distribution study, Fuel 225 (2018)
723 322-335.
724 [30] D. Mylaraswamy, DKit: A Blackboard-Based, Distributed, Multi-Expert
725 Environment for Abnormal Situation Management, West Lafayette: Purdue
726 University, 1996. (Ph.D. thesis)